Journal of Geodetic Science

• 1(4) • 2011 • 314-323 DOI: 10.2478/v10156-011-0011-1 •

Single Frequency Ionosphere-free Precise Point Positioning: A Cross-correlation Problem?

Research article

S. Choy[1]*, D. Silcock[1]

1 School of Mathematical and Geospatial Sciences, Royal Melbourne Institute of Technology (RMIT) University, GPO Box 2476V, Melbourne, Victoria 3001, Australia

Abstract:

This research investigates the feasibility of applying the code and the ionosphere-free code and phase delay observables for single frequency Precise Point Positioning (PPP) processing. Two observation models were studied: the single frequency ionosphere-free code and phase delay, termed the quasi-phase observable, and the code and quasi-phase combination. When implementing the code and quasi-phase combination, the cross-correlation between the observables must be considered. However, the development of an appropriate weight matrix, which can adequately describe the noise characteristics of the single frequency code and quasi-phase observations, is not a trivial task. The noise in the code measurements is highly dependent on the effects of the ionosphere; while the quasi-phase measurements are basically free from the effects of the ionospheric error. Therefore, it is of interest to investigate whether the correlation between the two measurements can be neglected when the code measurements were re-introduced to constrain the initial parameters estimation and thereby improving the phase ambiguities initialization process. It is revealed that the assumed uncorrelated code and quasi-phase combination provided comparable if not better positioning precision than the quasi-phase measurement alone. The level of improvement in the estimated positions is between 1 — 18 cm RMS.

Keywords:

single frequency • PPP • GPS • cross-correlation • code • ionosphere-free

Received 24-07-2011; accepted 07-09-2011

1. Introduction

Single frequency Precise Point Positioning (PPP) has received much attention from the worldwide Global Positioning System (GPS) research community (Beran 2008; Chen and Gao 2005; Le and Tiberius 2006; Simsky 2006). This technique is attractive because it offers a low-cost alternative to the popular differential positioning technique by providing comparable point positioning accuracy and precision. In a manner typical of all GPS positioning, PPP data are processed based on (weighted) least squares principle. This is where one needs to specify in terms of observations equations, the relationship between the observations and the unknown parameters, as well as the stochastic properties of observations that describe the precision of and correlation between observables. In practice, the estimation of the unknown parameters is complicated because observations are subject to noise, which affects the quality of the observations (Tiberius 1999). There have been numerous documented studies into single frequency PPP observations equations over recent years. However, research about the observations weight matrix has not attracted much attention from the wider GPS community. In fact, the proper choice of the observations weight matrix plays an equally crucial role in both adjusting and testing GPS data (Teunissen et al. 1998). This is because poor modeling of the observation weight can lead to non-optimal results and an incorrect interpretation of the solutions (Bona 2000).

The aim of this paper is to report on an investigation that was undertaken to address the stochastic properties of the observations weight matrix and specifically the presence of the cross-correlation between observables in the implemented single frequency PPP

*E-mail: suelynn.choy@rmit.edu.au

VERSITA

model. The single frequency PPP observation equations used in this research are based on the combination of the code and the ionosphere-free code and phase delay. For brevity, this combination is known as the *code and quasi-phase* combination. The quasi-phase is formed from the combination of the code and carrier phase measurements to alleviate the effects of the ionospheric error. As a result, cross-correlation is present between the two observables in the stochastic model, i.e. the code and the quasi-phase observables. However, this is not an issue if the mathematical model consists of only the quasi-phase observables, i.e. the single frequency ionosphere-free code and phase delay. In this case, the observation weight matrix can be treated as a diagonal matrix. The results from these two approaches have been evaluated and compared. The implications of these results will be discussed in detail.

It should be noted that a systematic study of the stochastic model is complex. This is because the noise characteristics depends not only on the measurements process and observation equations, but also the type and brand of the receiver used. Nevertheless, the focus of this study is mainly on the issues related to cross-correlation between the single frequency code and quasi-phase observables.

2. Single Frequency PPP Observation Equations

Single frequency PPP is based on un-differenced code and carrier phase data processing. If the antenna phase center offsets and variations, phase wind-up, relativistic errors, satellite hardware delay, and geophysical effects, such as site displacement effects, solid earth tides, and ocean loading have been correctly addressed (Kouba 2009); the satellite orbit and clock errors are eliminated by applying the available precise satellite orbit and clock corrections products (as with the case of all un-differenced PPP processing); and the tropospheric effects are modeled with sufficient accuracy using empirical models; then the measured code and carrier phase observation equations can be written as (1) and (2),

$$P_{L1} = \rho + cdt + d_{ion} + \varepsilon_{P_{L1}} \tag{1}$$

$$\Phi_{L1} = \rho + cdt - d_{ion} + \lambda_1 N_1 + \varepsilon_{\Phi_{L1}} \tag{2}$$

where, P_{L1} is the measured pseudorange on L1 (m), Φ_{L1} is the measured carrier phase on L1 (m), ρ is the true geometric range (m), c is the speed of light (ms^{-1}), dt is the receiver clock error (s), d_{ion} is the ionospheric delay (m), λ_1 is the wavelength on L1 (m), N_1 is the non-integer phase ambiguity on L1 (cycle), and $\varepsilon_{P_{L1}}$ and $\varepsilon_{\Phi_{L1}}$ is the code and carrier phase observation noise (m), respectively.

The mathematical implementation of the L1 quasi-phase observable, i.e. $\hat{\Phi}_{L1}$, is expressed as the simple average of (1) and (2),

$$\begin{aligned}\hat{\Phi}_{L1} &= \tfrac{P_{L1}+\Phi_{L1}}{2} \\ &= \rho + cdt + \tfrac{\lambda_1 N_1}{2} + \tfrac{\varepsilon_{P_{L1}}}{2} + \tfrac{\varepsilon_{\Phi_{L1}}}{2}\end{aligned} \tag{3}$$

Equation (3) is essentially the single frequency ionosphere-free code and phase delay proposed by Yunck (1993). The benefit of using the quasi-phase observables in single frequency PPP is apparent. The ionospheric error is effectively removed in the quasi-phase equation as a consequence of the opposite ionospheric effects on the code (delay) and carrier phase observations (advance). In other words, the ionospheric delay on the signal path is essentially eliminated using the quasi-phase observables.

In addition, the noise properties of the quasi-phase are mainly contributed by half of the code measurements noise, as in (3), and the phase measurements noise can be neglected as they are small, i.e. about a factor of 100 smaller than the code noise.

3. Adjustment Model

The adjustment model used in this research is based on a general least squares technique, which can adapt to varying user dynamics, i.e. static and kinematic (Tètreault et al. 2005). When simplified, the linearization of the observations equations (1) and (3) around the *a priori* parameters (x^0) and observations (l) becomes,

$$f(x^0, l) + B\Delta - v = 0 \tag{4}$$

where B is the design matrix, Δ is the vector of correction to the parameters x, $f(x^0, l)$ is the vector of observations, and v is the vector of residuals which contains the measurements noise (Kouba 2009).

In the case of a single frequency PPP processing model, there are three types of unknown parameters, i.e. receiver position (X^r,Y^r,Z^r), receiver clock corrections (dt), and non-integer phase ambiguities (N). The tropospheric Zenith Path Delay (ZPD) is compensated using an existing tropospheric model. Estimating the delay as part of the solutions would add strain to the solutions convergence time. Therefore, the tropospheric ZPD was not included as part of the single frequency least squares solution.

$$\mathbf{x} = \begin{bmatrix} X^r \\ Y^r \\ Z^r \\ dt \\ N^i \end{bmatrix}, \tag{5}$$

where (i=1, number of satellites)

The least squares estimation of the unknown parameters is given as (Kouba 2009),

$$\Delta = -(W_{xx} + B^T W B)^{-1} (B^T W f) \tag{6}$$

where W_{xx} is the *a priori* parameter weight matrix, and W is the *a priori* observations weight matrix. The *a priori* parameter weight matrix takes into account the variation in the parameters and the variances are updated between observation epochs.

4. Characteristics of the Code and Quasi-phase Measurements Noise

An indication of the noise characteristics of the code and quasi phase measurements can be obtained from an analysis of an appropriately constructed time series of the data. The data were measured at 30-second interval, and the code measurements were processed independently from the quasi-phase measurements.

In single frequency GPS code-only processing, the observation equation for the code measurement is shown in (1). For single frequency GPS users, the ionospheric delay can be corrected by applying appropriate correction models, such as the broadcast Klobuchar model (Klobuchar 1987) or the combined Global Ionosphere Maps (GIM) produced by the International GNSS Service (IGS). It should be noted that the ionosphere is highly unpredictable and as a result even the best computationally intensive models can only remove 70 — 80% RMS of the ionospheric delay. This means that the noise in the code observations may contain residual ionospheric error even after applying a correction model.

In this analysis, the ionospheric delay in the code measurements is corrected using the daily combined IGS *Final* GIM, which is accurate to 2 — 8 TECU (1 TECU corresponds to a delay of 0.16 m on L1 frequency). For more information about the GIM, refer to the IGS website (http://igscb.jpl.nasa.gov/). On the other hand, the quasi-phase measurements are free from the effects of the ionosphere.

Figure 1 shows an example of the code and quasi-phase measurements noise observed from a satellite (PRN 21) on DOY 185 2006 over a 4-hour period. The first figure illustrates a time series of the code noise and the second depicts the quasi-phase noise. These two measurements were processed independently. These first two time series give an indication of the code and quasi-phase noise and their corresponding variances $\sigma^2_{P_{L1}}$ and $\sigma^2_{\hat{\Phi}_{L1}}$. The third time series illustrates the difference between half the code noise minus the quasi-phase noise, i.e. $\Delta = \frac{P_{L1}}{2} - \hat{\Phi}_{L1}$. Using the propagation of variances, the variance of the difference can be expressed as,

$$\sigma^2_{\Delta} = \frac{1}{4}\sigma^2_{P_{L1}} - \sigma_{P_{L1}\hat{\Phi}_{L1}} + \sigma^2_{\hat{\Phi}_{L1}} \tag{7}$$

If $\sigma_{P_{L1}\hat{\Phi}_{L1}} = 0$, assuming that the code and quasi-phase observables are independent and uncorrelated, it may be expected that the noise in the code and quasi-phase difference to be larger than the noise in either the code or the quasi-phase measurements. This is, however, not the case. The noise of the code and quasi-phase difference is in fact smaller than either of the two measurements noise indicating the presence of correlation between the two measurements.

To quantify the code and quasi-phase noise characteristics in this particular case study, the data are used to estimate the code and quasi-phase variance covariance matrix and its inverse, i.e. the weight matrix. The estimated matrix reads,

$$Q_{P_{L1}\hat{\Phi}_{L1}} = \begin{bmatrix} 0.018 & 0.005 \\ 0.005 & 0.005 \end{bmatrix} \tag{8}$$

where the unit of the matrix entries are expressed in m^2. The variance covariance matrix is clearly not diagonal. The variance of the code measurements is about four times larger than the quasi-phase measurements variance. This confirms the fact that the quasi-phase observable exhibits a noise with a standard deviation (σ) of approximately half of the code noise and carrier phase noise, which has been demonstrated by Montenbruck (2003) and as expressed in (9). The quasi-phase observable is 'noisier' than the original carrier phase due to the influence of the code observations.

$$\sigma_{\widehat{\Phi}_{L1}} = \frac{1}{2}\sqrt{\sigma^2_{P_{L1}} + \sigma^2_{\Phi_{L1}}} \tag{9}$$

In fact, the quasi-phase measurement variance should be at least four times smaller than the code observation variance.

Due to the unresolved ambiguities in the initial PPP solutions, the time series of the initial solutions are too noisy for the estimation of a clear correlation between the code and quasi-phase observables. Once the quasi-phase ambiguities have stabilized, the noise in the solutions is half that of the code observable.

The calculated correlation matrix is,

$$R_{P_{L1}\hat{\Phi}_{L1}} = \begin{bmatrix} 1 & 0.480 \\ 0.480 & 1 \end{bmatrix} \tag{10}$$

This case study has confirmed that the variance covariance matrix is not a diagonal matrix; and the correlation coefficient matrix shows that there is a positive correlation between the two observables.

5. Correlation Coefficients

Consequently, if the code and the quasi-phase observables are used as a vector of observations, as in (4), then cross-correlation is introduced. In this case, the relationship between the code and quasi-phase observables needs to be described in the variance covariance matrix. The quasi-phase observables are linearly correlated with the code observations and are not stochastically independent. Using propagation of variances, the variance covariance matrix of the *code and quasi-phase* combination can be expressed mathematically as,

$$\begin{aligned} Q_{P_{L1}\hat{\Phi}_{L1}} &= \begin{bmatrix} \sigma^2_{P_{L1}} & \frac{1}{2}\sigma^2_{P_{L1}} \\ \frac{1}{2}\sigma^2_{P_{L1}} & \frac{1}{4}(\sigma^2_{P_{L1}} + \sigma^2_{\Phi_{L1}}) \end{bmatrix} \\ &\approx \begin{bmatrix} \sigma^2_{P_{L1}} & \frac{1}{2}\sigma^2_{P_{L1}} \\ \frac{1}{2}\sigma^2_{P_{L1}} & \frac{1}{4}\sigma^2_{P_{L1}} \end{bmatrix} \end{aligned} \tag{11}$$

It should be noted that the cross-correlation problem between the code and quasi-phase observables is not easily rectified due to the presence of the ionospheric error in the code measurements, while the quasi-phase measurements are basically free from the ionospheric delay (ignoring higher order ionospheric terms). This

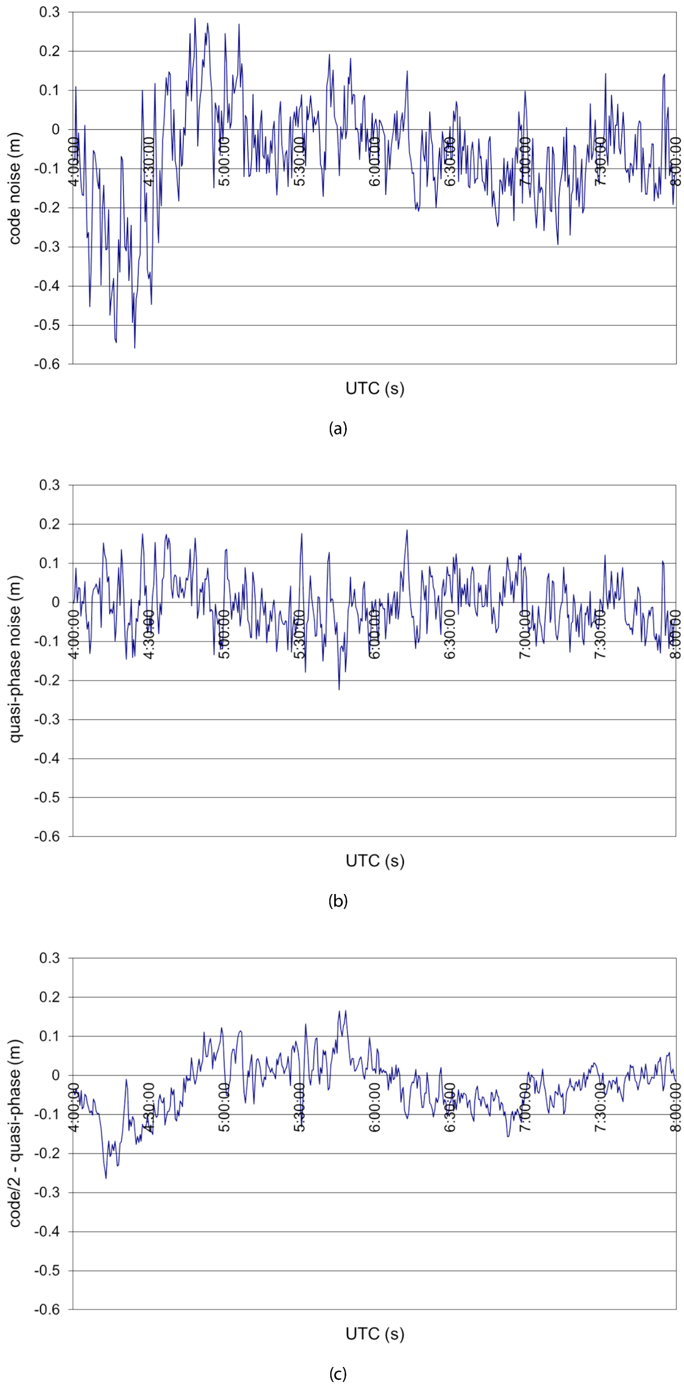

Figure 1. Time series of the code and quasi-phase noise.

makes it difficult to estimate the relative noise between the two measurements. In fact, the variance covariance matrix may not provide a realistic description of the noise characteristics of the *code and quasi-phase* combination. This is confirmed by the variations between (8) and (11). The estimated values in the variance covariance matrix vary depending on the location of the receiver, the ionospheric condition during which the data were collected, and the ionospheric model used in the code processing. Therefore, the observation system that incorporated the correlation coefficients may not be stable and the resultant estimated solutions are not optimal.

However, if only the quasi-phase measurements are used as observation vectors, then there is no issue of cross-correlation. In this case, the observation weight matrix is a diagonal matrix, which simplifies the stochastic process. Another alternative is to apply the *code and quasi-phase* combination and treat the observations as uncorrelated and as such the observation weight matrix in this combination is diagonal. The intention of re-introducing the code and assuming it to be uncorrelated to the quasi-phase measurements is to constrain initial parameters estimation process. This assists with the initialization of the phase ambiguities (Choy 2011). The results from these two approaches have been analyzed and compared. Table 1 identifies the processing approaches and their corresponding IDs (i.e. approach A and approach B) for discussions in the next section.

6. Data Processing and Results

Two IGS stations located in Australia were used in the analysis. These were Darwin (DARW) and Mount Stromlo (STR1). The stations were chosen because they represent the different latitudinal zones across Australia. DARW is located in the low latitude region, while STR1 is located in the middle latitude region. Although these stations are located on the Australian continent, the results would still serve as good representations of the achievable point positioning accuracy worldwide using these processing approaches.

These IGS stations are equipped with dual frequency geodetic quality GPS receivers. These receivers are able to deliver two different code measurements on L1 frequency, namely the C/A code (C1) and P code (P1). It is common to utilize the more precise P-code measurements in dual-frequency processing. However, for the purpose of this study, only C1 code observations on L1 were used in the single frequency data processing. This simulated using only a single frequency receiver.

Three consecutive days were randomly selected for each year starting from 2001 to 2006 (refer to Table 2). Table 2 also lists the ten centimeter radio flux (F10.7), and the geomagnetic planetary A index (Ap) indices for the selected days. These indices provide 'snapshots' of the global solar and geomagnetic activities, which in turn act as indicators of the level of disturbances in the ionosphere. All data sets used in this study were limited to the first 4 hours of the day, starting from 14:00 Local Time (LT), i.e. 14:00 to 18:00 LT. It is assumed that the daily maximum ionospheric activities occur at around 14:00 LT (Klobuchar 1987), and the effect of the ionosphere is at its peak during this period.

The most precise IGS *Final* orbit and satellite clock corrections were used in the data processing process to eliminate the satellite orbit and clock errors. This is to ensure that these errors are adequately removed and the remaining errors can be safely disregarded. For single frequency code and phase processing, it is recommended to model the tropospheric delay using an empirical model. This is because estimating the delay as part of the solution would add strain to the solution convergence time (Choy 2009). In addition, the induced error due to the delay (i.e. estimation or modeling) is in the level of a few centimeters, which is less than the observation noise and thus it could be ignored. In this study, the tropospheric delay was modeled using the Hopfield model with default atmospheric parameters, and the tropospheric ZPD was mapped to a slant delay by using the Niell mapping function. A cut-off elevation angle of 15° was used to reduce the data susceptibility to multipath effects. The observation interval of the collected data was 30 seconds. The satellite Differential Code Biases (DCBs) were taken into account in each of the data processing methods used because all included L1 code observations. The precise satellite clock correction products generated by the IGS always refer to the ionosphere-free linear combination between L1 and L2 frequencies, which are consistent with the P1 and P2 code measurements but not the C1 code. As a result, single frequency C1 users must apply the satellite DCBs in order to be consistent with satellite clock corrections convention. Refer to Schaer (1999) for a detailed description of the DCBs and their appropriate usage.

In approach A, the singularity of the normal equation is treated by implementing a sequential filter whereby information is passed on from one epoch to the next and the filter is initialized by an *a priori* variance covariance matrix. The rank deficiency problem is handled by additional *a priori* information on the observation biases. An approximate value of $0.5(P_{L1} - \Phi_{L1})$ can be obtained from the difference between the code and carrier phase measurement, ignoring the ionospheric range delay. An uncertainty of less than $10 - 20$ m may be assumed (Montenbruck, priv. comm.). In this case, any errors in the *a priori* information will be absorbed by the receiver clock solutions, and the position parameters are largely unaffected by these errors.

In approach B, the key element in achieving the best possible point positioning solutions is to assign a realistic *a priori* observations variance or sigma (standard deviation) ratio in the stochastic model. The purpose of this is to adequately reflect the relative weight and noise of the observations. The application of the *a priori* sigmas to the traditional dual frequency ionosphere-free linear combination follows the 'standard' nominal values widely used in GPS processing, i.e. the carrier phase is 100 times more precise than the code measurements (Kouba 2009). However, in the single frequency *code and quasi-phase* combination, assigning realistic *a priori* information is not as obvious because it uses both the code and quasi-phase observations. An empirical approach was adopted as part of this research to study the influence of different *a priori* observation sigma ratios on the quality of the estimated solutions. Table 3 outlines the different sigma ratios tested.

Table 1. Processing approaches (ID: A and B) tested in this study.

ID	Approach	Obs
A	Single frequency code and phase linear combination	$\hat{\Phi}_{L1}$
B	*Code and quasi-phase* combination	P_{L1} and $\hat{\Phi}_{L1}$

Table 2. The DOY, F10.7 and Ap indices of the selected days. *Source* http://wdc.kugi.kyoto-u.ac.jp/index.html; http://www.swpc.noaa.gov/ftpdir/indices/old_indices/

Year	DOY	F10.7	Ap
2002	274, 275, 276	105, 99, 81	67, 53, 45
2003	359, 360, 361	139, 137, 127	5, 8, 11
2004	153, 154, 155	90, 90, 90	16, 10, 8
2005	149, 150, 151	93, 95, 96	20, 90, 14
2006	183, 184, 185	87, 86, 88	2, 2, 12

Figures 2 and 3 depict the east, north and height errors in meters as a function of time for DARW and STR1 stations, respectively. The positioning errors were computed based on the differences between the known coordinates with the estimated values. These errors provide an indication of the achievable positioning accuracy using the different processing techniques. The published International Terrestrial Reference Frame (ITRF) coordinates obtained from the ITRF website (http://itrf.ensg.ign.fr/) were employed as reference points and assumed 'truth'. All the ITRF coordinates that were used as reference coordinates have also been brought forward to respective epochs. These figures are divided into five rows and three columns. Each row shows the positioning errors based on the different processing methods; each column consists of graphics showing the errors in the east, north and height components.

From Figures 2 and 3, it can be seen that the point positioning errors from approach B varied when the different a priori observation sigma ratios were applied. It can be deduced from the positioning results that approach B ($\approx$ 1:50) has a better overall performance and the solutions converged quicker than the other sigma ratios tested, i.e. 1:100 and 1:10. When an a priori code and quasi-phase sigma ratio of about 1:50 was used, the variability of the horizontal and height positioning errors was lower compared to observations sigma ratios of 1:100 and 1:10. Although this pattern was consistent at the two GPS stations located in different zones of latitude, remarkable improvement can be seen through the height component at DARW station.

The east, north and height estimations from approach B ($\approx$ 1:50) were quite similar to that of approach A. Both approaches required about half an hour to an hour for the solutions to converge within 1 m of the known values, although the convergence time of approach B was slightly shorter than approach A. On closer inspection of the initial positioning errors prior to solution convergence, approach B ($\approx$ 1:50) provided more accurate position estimates than approach A. However, once the solutions converged, the quality of the solutions from both methods was indeed comparable as the solutions were dominated by the single frequency ionosphere-free linear combination. Both methods could provide point positioning accuracy of better than 1 m.

The mean and RMS of the estimated positioning errors for each station were calculated and summarized in Table 4. The computed mean and RMS values for only approaches A and B ($\approx$ 1:50) were presented. The single frequency solutions from approach B were more precise than those of approach A. An improvement of 1 — 18 cm RMS in all positioning components was obtained. In fact, the level of improvement provided when using approach B was more apparent in the east and height components at DARW station. This indicates that the re-introduction of the code measurements in the observation model could help to constrain the initial parameters estimation process thus improving the precision of the solutions. This may be true especially for receivers located in the low or near equatorial region, and also during an ionospheric disturbed period.

7. Discussion and Conclusion

Since the quasi-phase was derived from the combination of the code and carrier phase measurements, the re-introduction of the raw code measurements in the observation model created a cross-correlation problem which needed to be considered stochastically. However, the cross-correlation problem between the code and quasi-phase observables was not easy to solve. This is due to the presence of the ionospheric errors in the code measurements, while the quasi-phase measurements are free from the ionospheric delay (ignoring higher order ionospheric terms). The results from a simple analysis revealed that the estimated variance covariance matrix did not conform to the mathematically derived matrix containing only

Table 3. The *a priori* code and quasi-phase sigmas (standard deviations) and their corresponding ratios used in approach B, i.e. the *code and quasi-phase* combination.

A Priori **Code Sigma**	*A Priori* **Quasi-Phase Sigma**	**Sigma Ratio**
4 m	0.03 m	≈ 1 : 100
4 m	0.10 m	≈ 1 : 50
4 m	0.30 m	≈ 1 : 10

Table 4. The positioning mean and RMS in m at DARW and STR1 stations based on approach A as well as approach B with an observation sigma ratio of ≈1:50.

	DARW, Mean (m)		**STR1, Mean (m)**	
ID	**A**	**B (≈1:50)**	**A**	**B (≈1:50)**
E	0.03	-0.07	-0.06	0.04
N	0.19	0.19	0.12	0.13
H	-0.31	-0.15	0.05	0.06
	DARW, RMS (m)		**STR1, RMS (m)**	
E	0.57	0.39	0.25	0.16
N	0.37	0.35	0.25	0.26
H	0.91	0.75	0.39	0.36

algebraic correlation. In fact, the mathematically derived variance covariance matrix may not imply a realistic description of the noise characteristics of the *code and quasi-phase* combination. In some circumstances, the computed solutions using the derived variance covariance matrix could be meaningless.

For this reason, it was suggested to utilize only the quasi-phase measurements, which are the single frequency code and phase delay, as the observation vector in the adjustment model. In this case, the observation weight matrix is a diagonal matrix implying that the quasi-phase measurements are uncorrelated. The feasibility of using this approach was tested as approach A in this study. The accuracy and precision of estimated solutions from this approach ranged between a few centimeters and a maximum of 1 m.

Another approach that was tested as part of this research was the *code and quasi-phase* combination, but the correlation between the measurements was ignored. This processing method is termed approach B in this study. The intention of re-introducing the assumed uncorrelated code measurements back into the observation model was to assist with the initialization of the phase ambiguities, and also to bridge over periods when the phase observation was not available or interrupted (e.g. cycle slips). In approach B, the balance between the relative weights (i.e. sigma ratio) of the observations was the key to achieving the best possible precision in the computed solutions.

Three sigma ratios were tested in this study. It was found that an observations sigma ratio of 1:50 provided optimal performance in terms of positioning accuracy, precision and also the convergence time despite the ionospheric conditions and the location of the GPS receivers. Furthermore, this processing strategy (i.e. approach B) provided more precise solutions (1 — 18 cm RMS) than just the approach A. The re-introduction of the code measurements constrained the initial parameters estimation process thus assisting with phase ambiguities initialization. Thus by treating the code and quasi-phase as two independent measurements, the code-based solution has a major impact on the initial portion of the solutions. In other words, the processing in approach B began with code measurements, then the phase measurements were gradually phased in, and at the same time, the float ambiguities converged to constant values. After the phase ambiguities stabilized, the ionosphere-free quasi-phase measurements dominated the solutions, and the code only had a marginal influence in the estimation process. The phase processing in approach B effectively absorbed the long-term code range biases into phase ambiguities given enough redundancy of measurements. Consequently, the solutions after convergence from this processing strategy were comparable to those from approach A. Both approaches provided decimeter-level point positioning accuracy and precision after solution convergence.

This paper has described a simple approach to study the cross-correlation between observables using the *code and quasi-phase* combination in single frequency PPP. Although the two measurements are highly correlated, it was found that the correlation can be safely neglected and the code measurements can be used to constrain the initial parameter estimation process thus improving the overall precision of the estimated solutions. The analysis has shown that it is possible to neglect the correlation between the

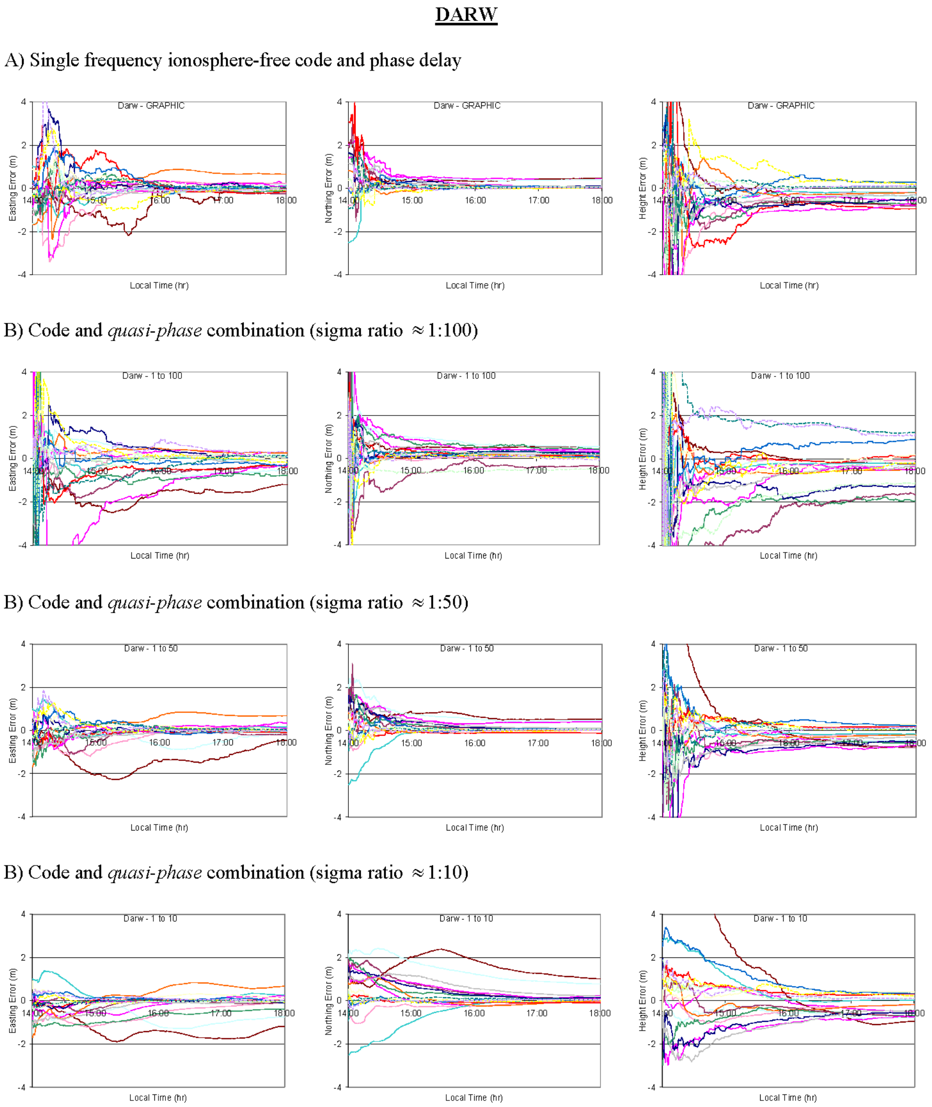

Figure 2. East, north and height positioning errors at DARW station using differing processing methods.

two measurements and still achieve comparable or better results with the single frequency ionosphere-free code and phase delay, i.e. the quasi-phase only method. Therefore, the assumed uncorrelated *code and quasi-phase* combination can be adopted in the un-differenced single frequency PPP processing. However, it is important to assign a realistic *a priori* observation weight that can adequately reflect the relative weighting or noise characteristics of the two measurements. It is the balance between the relative weights that ensures the best possible quality in the computed solutions.

Acknowledgements

The authors would like to thank the Geodetic Survey Division of Natural Resources Canada for kindly providing the Canadian Spatial Reference System-PPP (CSRS-PPP) software package, which was modified for this research. Also, the authors would like to thank Mr. Rodney Deakin and Dr. Babak Abbasi from RMIT University for their guidance and valuable discussion regarding this research work.

STR1

A) Single frequency ionosphere-free code and phase delay

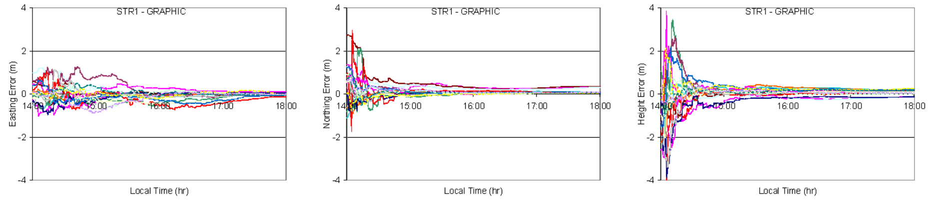

B) Code and *quasi-phase* combination (sigma ratio ≈1:100)

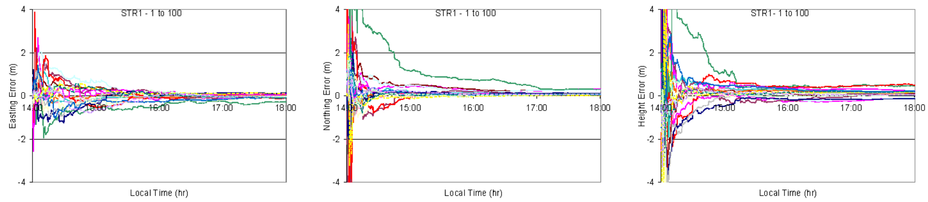

B) Code and *quasi-phase* combination (sigma ratio ≈1:50)

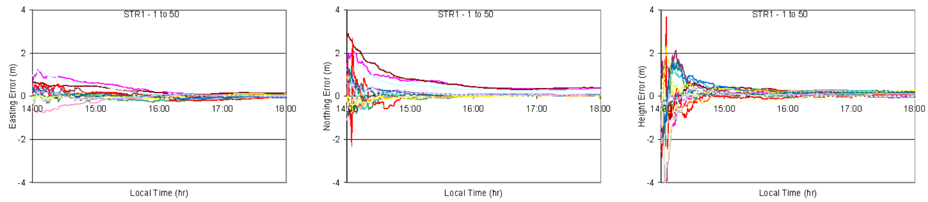

B) Code and *quasi-phase* combination (sigma ratio ≈1:10)

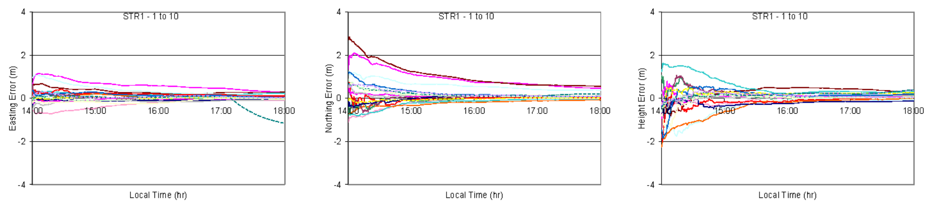

Figure 3. East, north and height positioning errors at STR1 station using differing processing methods.

References

Abdel-salam, M., 2005, Precise Point Positioning Using Un-Differenced Code and Carrier Phase Observations, PhD thesis, The University of Calgary, Canada

Beran, T., 2008, Single-frequency, Single-receiver Terrestrial and Spaceborne Point Positioning, PhD thesis, University of New Brunswick, Frederiction, New Brunswick, Canada

Bona, P., 2000, Precision, Cross Correlation, and Time Correlation of GPS Phase and Code Observations, GPS Solut, 4(2), 3-13, doi:10.1007/PL00012839

Chen, K., and Gao, Y., 2005, Real-Time Precise Point Positioning Using Single Frequency Data, Proceedings of ION GNSS 18th International Technical Meeting of the Satellite Division, Long Beach, CA, 1514-1523

Choy, S., 2011, High Accuracy Precise Point Positioning Using a Single Frequency GPS Receiver, J Appl Geodes, in press, doi:10.1515/JAG.2011.008

Choy, S., 2009, An Investigation into the Accuracy of Single Frequency Precise Point Positioning, PhD thesis, RMIT University, Melbourne, Australia

Klobuchar, J. A., 1987, Ionospheric Time-Delay Algorithm for Single-Frequency GPS Users, IEEE Trans on Aerospace Electron

Syst, AES-23(3), 325-331

Kouba, J., 2009, A Guide to using International GPS Service (IGS) Products, Tech. rep., International GNSS Service

Le, A. Q., and Tiberius, C. C. J. M., 2006, Single-Frequency Precise Point Positioning with Optimal Filtering, GPS Solut, 11(1), 61-69

Montenbruck, O., 2003, Kinematic GPS Positioning of LEO Satellites using Ionosphere-Free Single Frequency Measurements, Aerosp Sci Technol, 7, 396-405

Schaer, S., 1999, Mapping and Predicting the Earth's Ionosphere using the Global Positioning System, PhD thesis, University of Berne, Switzerland

Simsky, A., 2006, Standalone Real-Time Navigation Algorithm for Single-Frequency Ionosphere-Free Positioning Based on Dynamic Ambiguities (DARTS-SF), Proceedings of ION GNSS 18th International Technical Meeting of the Satellite Division, Fort Worth, Texas, 301-308

Tètreault, P., Kouba, J., Hèroux, P., and Legree, P., 2005, CSRS-PPP: An internet service for GPS user access to the Canadian Spatial Reference Frame, GEOMATICA, 59(1), 17-28

Teunissen, P., Jonkman, N., and Tiberius, C. C. J. M., 1998, Weighting GPS Dual Frequency Observations: Bearing the Cross of Cross-Correlation, GPS Solut, 2(2), 28-37

Tiberius, C. C. J. M., 1999, The GPS Data Weight Matrix: What Are the Issues?, Proceedings of ION 1999 National Technical Meeting "Vision 2010: Present and Future", San Diego, California, USA, 219-227

Yunck, T., 1993, Coping With the Atmosphere and Ionosphere in Precise Satellite and Ground Positioning, Geophys Monogr, (73)13

Zumberge, J. F., Heflin, M. B., Jefferson, D. C., Watkins, M. M., and Webb, F. H., 1997, Precise Point Positioning for The Efficient and Robust Analysis of GPS Data From Large Networks, J Geophys Res, 102(B3), 5005-5017